Eur J Nucl Med Mol Imaging (2010) 37:1345–1355
DOI 10.1007/s00259-009-1363-y

ORIGINAL ARTICLE

^{68}Ga-labelled exendin-3, a new agent for the detection of insulinomas with PET

Maarten Brom · Wim J. G. Oyen · Lieke Joosten · Martin Gotthardt · Otto C. Boerman

Received: 29 July 2009 / Accepted: 10 December 2009 / Published online: 29 January 2010

Abstract
Purpose Insulinomas are neuroendocrine tumours derived from pancreatic β-cells. The glucagon-like peptide 1 receptor (GLP-1R) is expressed with a high incidence (>90%) and high density in insulinomas. Glucagon-like peptide 1 (GLP-1), the natural ligand of GLP-1R, is rapidly degraded in vivo. A more stable agonist of GLP-1R is exendin-3. We investigated imaging of insulinomas with DOTA-conjugated exendin-3 labelled with ^{68}Ga.
Methods Targeting of insulinomas with [Lys^{40}(DOTA)]exendin-3 labelled with either ^{111}In or ^{68}Ga was investigated in vitro using insulinoma tumour cells (INS-1). [Lys^{40}(^{111}In-DTPA)]Exendin-3 was used as a reference in this study. In vivo targeting was investigated in BALB/c nude mice with subcutaneous INS-1 tumours. PET imaging was performed using a preclinical PET/CT scanner.
Results In vitro exendin-3 specifically bound and was internalized by GLP-1R-positive cells. In BALB/c nude mice with subcutaneous INS-1 tumours a high uptake of [Lys^{40}(^{111}In-DTPA)]exendin-3 in the tumour was observed (33.5±11.6%ID/g at 4 h after injection). Uptake was specific, as determined by coinjection of an excess of unlabelled [Lys^{40}]exendin-3 (1.8±0.1%ID/g). The pancreas also exhibited high and specific uptake (11.3±1.0%ID/g). High uptake was also found in the kidneys (144±24%ID/g) and this uptake was not receptor-mediated. In this murine tumour model optimal targeting of the GLP-1R expressing tumour was obtained at exendin doses ≤0.1 μg. Remarkably, tumour uptake of ^{68}Ga-labelled [Lys^{40}(DOTA)]exendin-3 was lower (8.9±3.1%ID/g) than tumour uptake of ^{111}In-labelled [Lys^{40}(DTPA)]exendin-3 (25.4±7.2%ID/g). The subcutaneous tumours were clearly visualized by small-animal PET imaging after injection of 3 MBq of [Lys^{40}(^{68}Ga-DOTA)]exendin-3.
Conclusion [Lys^{40}(^{68}Ga-DOTA)]Exendin-3 specifically accumulates in insulinomas, although the uptake is lower than that of [Lys^{40}(^{111}In-DTPA)]exendin-3. Therefore, [Lys^{40}(^{68}Ga-DOTA)]exendin-3 is a promising tracer to visualize insulinomas with PET.

Keywords Insulinoma · GLP-1 receptor · Imaging · SPECT · PET · Exendin

M. Brom (✉) · W. J. G. Oyen · L. Joosten · M. Gotthardt · O. C. Boerman
Department of Nuclear Medicine,
Radboud University Nijmegen Medical Centre,
PO Box 9101, 6500 HB Nijmegen, The Netherlands
e-mail: m.brom@nucmed.umcn.nl

Introduction

Insulinomas are neuroendocrine tumours (NET) derived from pancreatic beta-cells. The diagnosis is based on clinical symptoms (such as neuroglycopenic symptoms) and biochemical parameters (endogenous hyperinsulinism confirmed by hypoglycaemia). The standard treatment for insulinomas is surgical resection, requiring exact localization of the tumour lesions. Therefore, patients usually undergo computed tomography (CT) and magnetic resonance imaging (MRI) to precisely localize the primary tumour and potential metastases in those with malignant insulinoma. Somatostatin receptor scintigraphy (SRS) is considered the most sensitive method for detection of NET [1]. In contrast to other NET, the sensitivity of SRS for detecting insulinomas is only 40–60% due to the relatively low incidence of somatostatin subtype receptor (sstr) 2 and sstr5 expression in insulinomas [1–3]. Therefore, SRS is not suitable for localizing insulinomas. Recent studies have shown a high detection rate of insulinomas with endoscopic

ultrasonography [4]. However, the high detection rate is limited to tumours that are located in the head and the body of the pancreas. Moreover, this technique requires specialized expertise and is observer-dependent. Angiography shows reasonable localization of insulinomas in approximately 70% of patients. However, the localization varies from 43% to 94% due to observer-dependency [5]. Arterial stimulation and venous sampling is a sensitive method that is able to localize over 90% of insulinomas [5]. The major drawback is that the procedure is invasive. Thus, there is a need for new noninvasive strategies for localization of insulinomas.

The glucagon-like peptide 1 receptor (GLP-1R) is expressed in >90% of insulinomas at a mean density twice that of sstr2 [6]. First preclinical studies have shown that ^{123}I-GLP-1 and ^{123}I-exendin-3 accumulate in rat insulinomas (RINm5F) subcutaneously implanted in NEDH rats, and that these tumours can be detected scintigraphically [7]. However, radioiodinated peptides have a relatively low uptake in vivo, due to washout of the radionuclide after internalization [8–11]. Recent studies have shown high uptake of DTPA-conjugated [Lys^{40}]exendin-4 labelled with ^{111}In in the Rip1Tag2 spontaneous insulinoma mouse model [12, 13]. Moreover, administration of a therapeutic dose of ^{111}In-labelled [Lys^{40}(DTPA)]exendin-4 markedly inhibited the growth of insulinomas in Rip1Tag2 mice [14]. Based on these promising results, ^{111}In-labelled exendin-4 has been used for the detection of insulinomas in humans by single photon emission computed tomography (SPECT) [15]. Previous studies have used exendin-3 and exendin-4, which share 95% homology (Table 1). Exendin-3 and exendin-4 differ in two amino acids (positions 2 and 3) located in the region of the peptide that is involved in internalization of the receptor–ligand complex, which might lead to differences in biodistribution of these peptides. In this study we therefore compared the biodistribution of [Lys^{40}(DTPA)]exendin-3 and [Lys^{40}(DTPA)]exendin-4 labelled with ^{111}In.

Because even small insulinomas may induce clinical symptoms, imaging methods for the detection of these tumours needs to be highly sensitive. Positron emission tomography (PET) may therefore offer an advantage over SPECT because of its excellent sensitivity in combination with its improved spatial resolution. As the radionuclide for PET imaging of GLP-1Rs with exendin, ^{68}Ga seems to be the optimal candidate since DOTA-conjugated probes can be rapidly and efficiently labelled with ^{68}Ga, and because ^{68}Ga is a generator-produced positron emitter, it is widely available and relatively cheap. The conjugation of exendin-3 with DOTA could change the pharmacokinetics of the peptide. Therefore we compared the biodistribution of [Lys^{40}(DTPA)]exendin-3 and [Lys^{40}(DOTA)]exendin-3 labelled with ^{111}In.

We determined the potential of ^{68}Ga-labelled [Lys^{40}(DOTA)]exendin-3 for insulinoma imaging. [Lys^{40}(^{111}In-DTPA)]exendin-4 was successfully used for this application [12, 14, 15]. Here, biodistributions of [Lys^{40}(^{111}In-DTPA)]exendin-3 and [Lys^{40}(^{111}In-DTPA)]exendin-4 were compared. The effect of the chelator (DOTA or DTPA) was examined by comparing the biodistributions of [Lys^{40}(^{111}In-DTPA)]exendin-3 and [Lys^{40}(^{111}In-DOTA)]exendin-3. The biodistributions of ^{68}Ga- and ^{111}In-labelled exendin-3 were compared. Finally, microPET images were acquired of insulinoma-bearing BALB/c nude mice after injection of [Lys^{40}(^{68}Ga-DOTA)]exendin-3.

Materials and methods

Peptides and radionuclides

[Lys^{40}(DOTA)]exendin-3, [Lys^{40}(DTPA)]exendin-3 and [Lys^{40}(DTPA)]exendin-4 were purchased from Peptide Specialty Laboratories (Heidelberg, Germany). The DTPA or DOTA was conjugated to the ε-amino group of the lysine (K40) and the C-terminal carboxyl group was amidated. The structures of [Lys^{40}(DTPA)]exendin and Lys^{40}(DOTA)]exendin are shown in Fig. 1. $^{111}InCl_3$ was obtained from Covidien (Petten, The Netherlands). $^{68}GaCl_3$ was eluted from a TiO_2-based 1,110 MBq ^{68}Ge/^{68}Ga generator (Obninsk, Russia) with 0.1 *N* Ultrapure HCl (J.T. Baker, Deventer, The Netherlands).

Radiolabelling

[Lys^{40}(DTPA)]Exendin-3 was dissolved in 0.1 *M* MES (2-(*N*-morpholino)ethanesulphonic acid) buffer, pH 5.5, and 150 MBq ^{111}In was added to 1 μg peptide followed by five volumes of 0.1 *M* MES buffer, pH 5.5, resulting in a total volume of reaction mixture ranging from 800 μl to 2,345 μl. After incubation at room temperature for 30 min, quality control was performed using reversed-phase high-performance liquid chromatography (RP-HPLC) on a C_{18} reversed-phase column (Zorbax Rx-C18; 4.6 mm× 25 cm; Agilent Technologies) and instant thin-layer chroma-

Table 1 Amino acid structures of exendin-3 and exendin-4. Homologous amino acids are underlined

Peptide	Amino acid sequence
Exendin-3	HSDGTFTSDLSKQMEEEAVRLFIEWLKNGGPSSGAPPPS-NH2
Exendin-4	HGEGTFTSDLSKQMEEEAVRLFIEWLKNGGPSSGAPPPS-NH2

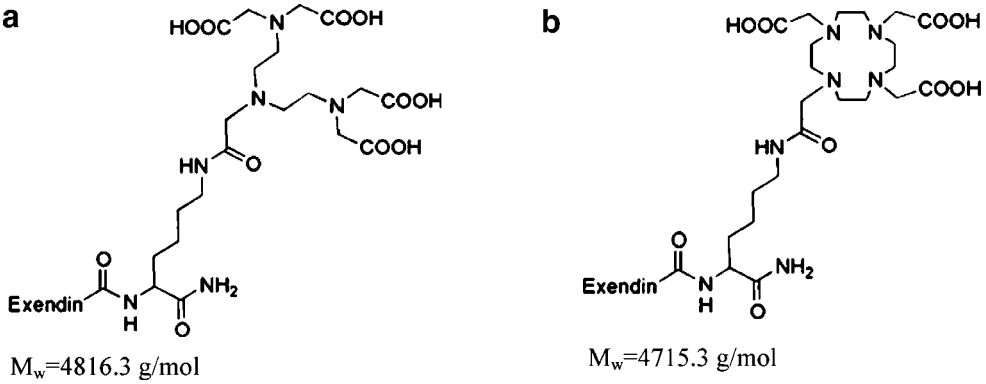

Fig. 1 Structures of [Lys^{40}(DTPA)]exendin-3 (**a**) and [Lys^{40}(DOTA)]exendin-3 (**b**)

tography (ITLC). The column was eluted with 10 m*M* ammonium acetate, pH 5.5, with a linear gradient from 3% to 100% acetonitrile in 10 min (flow rate 1 ml/min). ITLC was performed on silica gel ITLC (Pall Corporation Life Sciences, New York, NY). Two mobile phases were used: 0.1 *M* EDTA in 0.1 *M* NH_4Ac, pH 5.5 (R_f ^{111}In-labelled exendin = 0, R_f unbound ^{111}In = 1) and 0.25 *M* NH_4Ac (pH 5.5)/methanol (1:1) (R_f colloidal residues = 0: , R_f ^{111}In-labelled exendin and unbound ^{111}In = 1).

[Lys^{40}(DOTA)]Exendin-3 was labelled with ^{111}In by adding five volumes of 0.25 *M* ammonium acetate buffer, pH 5.5, containing 5 μg peptide and 55 MBq ^{111}In, resulting in a total volume of reaction mixture ranging from 359 μl to 1,043 μl. After 20 min incubation at 95°C, quality control was performed using RP-HPLC and ITLC as described above. [Lys^{40}(DOTA)]exendin-3 was labelled with ^{68}Ga by adding 185 MBq of ^{68}Ga in 350 μl 0.1 *N* Ultrapure HCl to 42 μl 2.5 *M* HEPES (4-(2-hydroxyethyl)-1-piperazineethanesulphonic acid) buffer, pH 7, containing 8 μg [Lys^{40}(DOTA)]exendin-3. The final pH of the reaction mixture was 3.0. The mixture was incubated at 95°C for 15 min, then EDTA was added to a final concentration of 5 m*M*, and the mixture was incubated at room temperature for 5 min. The reaction mixture was purified by HPLC using a C_8 reversed-phase column (Zorbax eclipse XDB C_8 4.6×150 mm, 5 μm; Agilent Technologies). The column was eluted with 10 m*M* ammonium acetate, pH 5.5 (0–5 min) and 40% ethanol (5–10 min) followed by a linear gradient from 40% to 90% ethanol over 5 min (flow rate 1 ml/min). The fractions containing [Lys^{40}(^{68}Ga-DOTA)] exendin-3 were collected and diluted with PBS containing 0.5% BSA to a final ethanol concentration of less than 10% before injection into mice (injection volume 0.2 ml). The contents of unincorporated ^{68}Ga and ^{68}Ga colloid in the purified ^{68}Ga-labelled [Lys40(DOTA)]exendin-3 preparations were determined using ITLC as described above.

Cell culture

The rat insulinoma cell line INS-1 [16] was maintained in RPMI-1640 medium supplemented with 10% fetal bovine serum, 2 m*M* glutamine, 10 m*M* HEPES, 50 μM β-mercaptoethanol, 1 m*M* sodium pyruvate, 100 U/ml penicillin and 100 μg/ml streptomycin, in a humidified atmosphere containing 5% CO_2 at 37°C. The cells were harvested by trypsinization with trypsin/EDTA.

IC_{50} determination

The 50% inhibitory concentrations (IC_{50}) of [Lys^{40}(^{nat}In-DTPA)]exendin-3, [Lys^{40}(^{nat}In-DOTA)]exendin-3 and [Lys^{40}(^{nat}Ga-DOTA)]exendin-3 were determined using suspensions of INS-1 cells. [Lys^{40}(DTPA)]Exendin-3 was labelled with stable ^{nat}In by adding 10.6 nmol $^{nat}InCl_3$ (Merck, Darmstadt, Germany) to 2.12 nmol [Lys^{40}(DTPA)] exendin-3 (0.21 nmol/μl) in 30 μl 0.1 *M* MES buffer, pH 5.5, and incubated at room temperature for 30 min. [Lys^{40}(DOTA)]Exendin-3 was labelled with ^{nat}In in 0.25 *M* NH_4Ac, pH 5.5, containing 2.12 nmol [Lys^{40}(DOTA)] exendin-3. After adding 10.6 nmol ^{nat}In, the reaction mixture was incubated at 95°C for 30 min. [Lys^{40}(DOTA)]exendin-3 was labelled with stable ^{nat}Ga by adding 10.6 nmol $^{nat}Ga(NO)_3$ (Sigma Aldrich, St Louis, MO) to 2.12 nmol [Lys^{40}(DOTA)]exendin-3 in 30 μl 0.25 *M* NH_4Ac, pH 5.5, followed by incubation at room temperature for 3 h. INS-1 cells were resuspended in binding buffer (HEPES-buffered RPMI containing 1% BSA) to a concentration of 3 million cells/0.5 ml. After 10 min incubation at 0°C, ^{nat}In- or ^{nat}Ga-labelled peptide was added to a final concentration in the range 0.10–350 n*M* along with radiolabelled [Lys^{40}(^{111}In-DTPA)]exendin-3 (60,000 dpm). To prevent internalization, cells were incubated on ice for 4 h. The cell suspension was centrifuged at 3,000 *g* for 5 min and the supernatant was discarded. The cells were washed twice with ice-cold PBS, centrifuged, and the radioactivity in the cell pellet was determined in a gamma-counter (Wizard, Wallac-Oy, Uppsala, Sweden), and the bound fraction was determined.

In vitro internalization

The kinetics of internalization of [Lys^{40}(^{111}In-DTPA)] exendin-3 were determined as described previously [17].

INS-1 cells were seeded at a density of 500,000 cells/well in six-well plates and incubated overnight at 37°C. The cells were washed twice with binding buffer and subsequently incubated at 37°C for 10 min in 1.0 ml binding buffer. Approximately 60,000 dpm of ^{111}In-labelled peptide (55 fmol) was added followed by incubation for 0.5, 1, 2 or 4 h at 37 C. To determine nonspecific binding, 1 μg unlabelled [Lys^{40}]exendin-3 was added together with the ^{111}In-labelled peptide to three wells per time point. After incubation, the cells were washed twice with binding buffer. To determine the surface-bound radiolabelled peptide, ice-cold acid buffer (0.1 *M* acetic acid, 154 m*M* NaCl, pH 2.5) was added and cells were incubated for 10 min at 4°C. After washing the cells twice with binding buffer, they were harvested with a cotton stick and the cell-associated activity was measured in a gamma-counter. The internalized fraction (cell-associated activity after acid wash) and the receptor-bound fraction (activity removed by acid wash) were determined. The values of the internalized and receptor bound fractions were corrected for nonspecific binding as determined by coincubation with an excess of unlabelled [Lys^{40}]exendin-3 (1 μg/well).

Biodistribution studies of [Lys^{40}(^{111}In-DTPA)]exendin-3 and [Lys^{40}(^{111}In-DTPA)]exendin-4

The biodistributions of [Lys^{40}(^{111}In-DTPA)]exendin-3 and [Lys^{40}(^{111}In-DTPA)]exendin-4 were compared. Female BALB/c nude mice at 6–8 weeks of age were injected subcutaneously in the right flank with 0.2 ml of a suspension of INS-1 cells containing 5×10^7 cells/ml. When the tumours were 2–5 mm in diameter, the mice were randomly divided into groups of five mice each. The mice were injected intravenously with 370 kBq (peptide dose 0.1 μg) of ^{111}In-labelled [Lys^{40}(DTPA)]exendin-3 (n=5) or ^{111}In-labelled [Lys^{40}(DTPA)]exendin-4 (n=5) via the tail vein. The mice were killed 4 h after injection by CO_2/O_2 suffocation, and blood, tumour and relevant tissues (muscle, heart, lung, spleen, pancreas, kidney, liver, stomach and duodenum) were removed, weighed and counted in a gamma-counter. The percentage injected dose per gram (%ID/g) was determined for each tissue. To determine whether the exendin uptake is GLP-1R-mediated, a 100-fold excess (10 μg) of unlabelled [Lys^{40}]exendin was coinjected in a separate group of two mice.

Biodistribution studies of [Lys^{40}(^{111}In-DTPA)]exendin-3 and [Lys^{40}(^{111}In-DOTA)]exendin-3

In order to determine the effect of the chelator, the biodistributions of [Lys^{40}(^{111}In-DTPA)]exendin-3 and [Lys^{40}(^{111}In-DOTA)]exendin-3 were determined in BALB/c nude mice with a subcutaneous tumour. The mice were injected intravenously with 370 kBq ^{111}In-labelled [Lys^{40}(DTPA)] exendin-3 (n=5) or [Lys^{40}(DOTA)]exendin-3 (n=5). To determine the GLP-1R-mediated uptake, a separate group of two mice were coinjected with an excess of unlabelled [Lys^{40}]exendin. The mice were killed 4 h after injection by CO_2 suffocation, and blood, tumour and major organs were removed, weighed and counted.

Biodistribution studies of [Lys^{40}(^{111}In-DTPA)]exendin-3 and [Lys^{40}(^{68}Ga-DOTA)]exendin-3

The biodistributions of [Lys^{40}(^{111}In-DTPA)]exendin-3 and [Lys^{40}(^{68}Ga-DOTA)]exendin-3 were determined in BALB/c nude mice with subcutaneous INS tumours. Mice were injected intravenously with 370 kBq ^{111}In (n=5) or 1 MBq ^{68}Ga-labelled exendin-3 (n=5) at a peptide dose of 0.1 μg. To determine the GLP-1R-mediated uptake, a separate group of two mice were co-injected with an excess of unlabelled [Lys^{40}]exendin. Another group of two mice were injected with [Lys^{40}(^{68}Ga-DOTA)]exendin-3 that was purified on a disposable PD10 column instead of by RP-HPLC. The mice were killed 1 h after injection by CO_2 suffocation, and blood, tumour and major organs were removed, weighed and counted.

Peptide dose-escalation study

To determine the optimal peptide dose of exendin-3 in this model for tumour imaging, BALB/c nude mice with a subcutaneous INS-1 tumour were injected intravenously with 370 kBq [Lys^{40}(^{111}In-DTPA)]exendin-3 (peptide dose 0.003 μg) and were coinjected with various amounts of unlabelled [Lys^{40}]exendin-3 to final peptide doses in the range 0.003–10.0 μg (five mice per peptide dose). The mice were killed 4 h after injection by CO_2/O_2 suffocation, and the radioactivity in the blood, tumour and relevant tissues was measured in a gamma counter.

PET imaging

PET images were acquired of BALB/c nude mice (n=3) with a subcutaneous INS-1 tumour in the hind limb using a small-animal PET/CT scanner (Inveon; Siemens Medical Solutions, Knoxville, TN). The scanner had an axial field of view of 12.7 cm and a 1.4-mm FWHM spatial resolution in images reconstructed using Fourier rebinning and filtered back projection. When the tumours had a diameter of 2–5 mm, the mice were injected intravenously via the tail vein with 3 MBq HPLC-purified [Lys^{40}(^{68}Ga-DOTA)]exendin-3 (specific activity 110 GBq at completion of the labelling, 50 GBq/μmol at time of injection) corresponding with an exendin dose of 0.3 μg. PET images were acquired 1 h after injection under isoflurane/O_2/N_2O inhalation anaesthesia.

The PET images were acquired over 45 min for the emission scan, and the images were reconstructed by OSEM3D/MAP reconstruction.

Results

Radiolabelling

Specific activities up to 700 GBq/μmol for [Lys^{40}(^{111}In-DTPA)]exendin-3 were obtained with a radiochemical purity exceeding 95%. [Lys^{40}(DOTA)]exendin-3 was labelled efficiently with ^{111}In and ^{68}Ga. Specific activities of 20 GBq/μmol with a radiochemical purity >95% as determined by HPLC were obtained for [Lys^{40}(^{111}In-DOTA)]exendin-3. [Lys^{40}(DOTA)]exendin-3 was labelled with ^{68}Ga with a specific activity of 110 GBq/μmol with a radiochemical purity >99% after HPLC purification. Without HPLC purification, a specific activity of 17 GBq/μmol was obtained. Unbound ^{111}In and ^{68}Ga eluted from the column after 3 min, whereas ^{111}In- and ^{68}Ga-labelled exendin had a retention time of about 13 min.

IC_{50} determination

The results of the IC_{50} determination are shown in Fig. 2. The IC_{50} for ^{nat}In-DTPA-[Lys^{40}]exendin-3, [Lys^{40}(^{nat}In-DOTA)]exendin-3 and [Lys^{40}(^{nat}Ga-DOTA)]exendin-3 for binding to INS-1 cells were 8.5 n*M* (95% confidence Interval 4.30 to 16.8 n*M*), 5.3 n*M* (95% confidence Interval 2.75 to 11.1 n*M*), and 5.7 n*M* (95% confidence Interval 2.91 to 11.3 n*M*), respectively; there was no significant difference among these IC_{50} values (p=0.5038 for log(IC_{50}) differences determined by the *F*-test).

Internalization kinetics

Figure 3 summarizes the internalization kinetics of [Lys^{40}(^{111}In-DTPA)]exendin-3 in INS-1 cells as determined in vitro. After 0.5 h, 0.1±0.03 fmol [Lys^{40}(^{111}In-DTPA)] exendin-3 was bound to the receptor and 0.4±0.01 fmol was internalized. After 4 h these values had increased to 2.6±0.04 and 3.9±0.06 fmol, respectively.

Biodistribution studies of [Lys^{40}(^{111}In-DTPA)]exendin-3, [Lys^{40}(^{111}In-DTPA)]exendin-4, and of [Lys^{40}(^{111}In-DOTA)] exendin-3

Figure 4 summarizes the biodistributions of [Lys^{40}(^{111}In-DTPA)]exendin-3 and [Lys^{40}(^{111}In-DTPA)]exendin-4. Both ^{111}In-labelled exendin-3 and exendin-4 showed high tumour uptake (36.0±5.4%ID/g and 36.3±8.0%ID/g). Coadministration of an excess of unlabelled [Lys^{40}]exendin-3 blocked the tumour uptake (1.2±0.3%ID/g and 1.0±0.4%ID/g, respectively; p<0.01), indicating that the uptake is GLP-1R-mediated. Specific uptake of [Lys^{40}(^{111}In-DTPA)]exendin-3 and [Lys^{40}(^{111}In-DTPA)]exendin-4 was also seen in the pancreas (p<0.01), lung (p<0.01) and stomach (p<0.01), but there was no significant difference in uptake in tumour, pancreas, lung or stomach. The renal uptake of [Lys^{40}(^{111}In-DTPA)]exendin-3 and [Lys^{40}(^{111}In–DTPA)]exendin-4 was 146.1±21.0%ID/g and 140.5±17.7%ID/g, and this was not blocked by an excess of unlabelled exendin-3, indicating that the uptake is not GLP-1R-mediated.

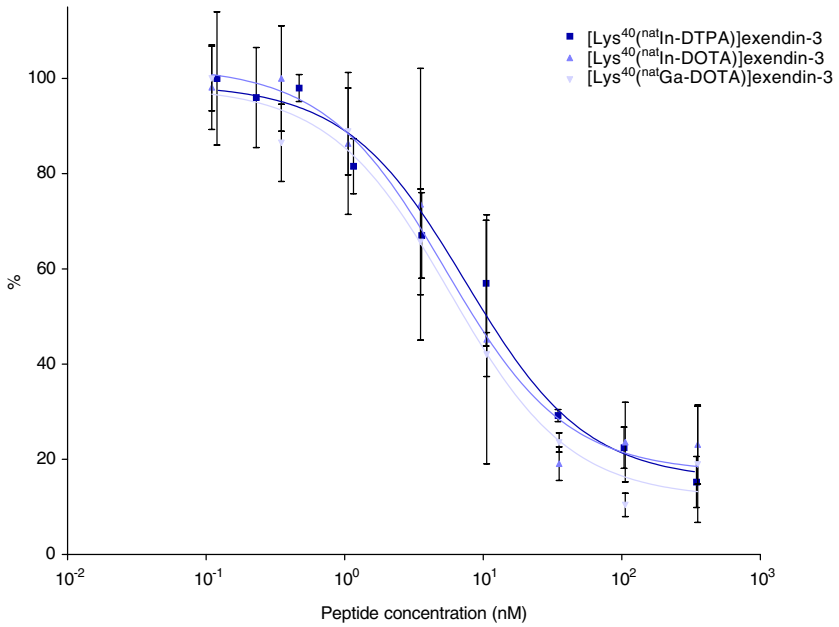

Fig. 2 Competition binding assay (IC_{50}) of [Lys^{40}(^{nat}In-DTPA)] exendin-3, [Lys^{40}(^{nat}In-DOTA)] exendin-3 and [Lys^{40}(^{nat}Ga-DOTA)]exendin-3 in INS-1 cells. [Lys^{40}(^{111}In-DTPA)]exendin-3 was used as tracer

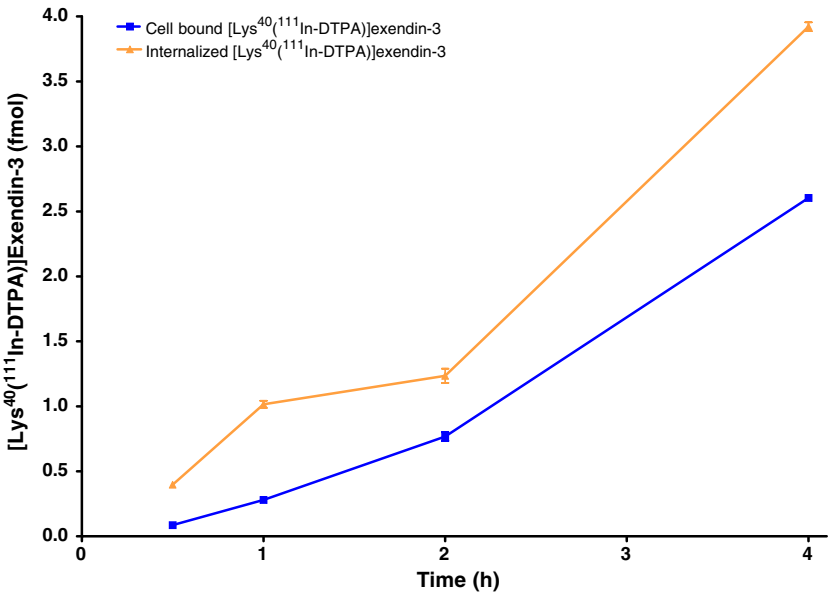

Fig. 3 In vitro internalization kinetics of [Lys^{40}(^{111}In-DTPA)] exendin-3 in INS-1 cells. The cell-bound and internalized fractions are corrected for non-specific binding and uptake determined by coincubation with an excess of unlabelled [Lys^{40}] exendin-3

The chelator did not affect the biodistribution of [Lys^{40}] exendin-3 as evidenced by the almost identical concentrations of [Lys^{40}(^{111}In-DOTA)]exendin-3 and [Lys^{40}(^{111}In-DTPA)]exendin-3 in all tissues examined (Fig. 5).

Biodistribution of [Lys^{40}(^{68}Ga-DOTA)]exendin-3

The biodistribution of [Lys^{40}(^{68}Ga-DOTA)]exendin-3 was determined 1 h after injection in BALB/c nude mice

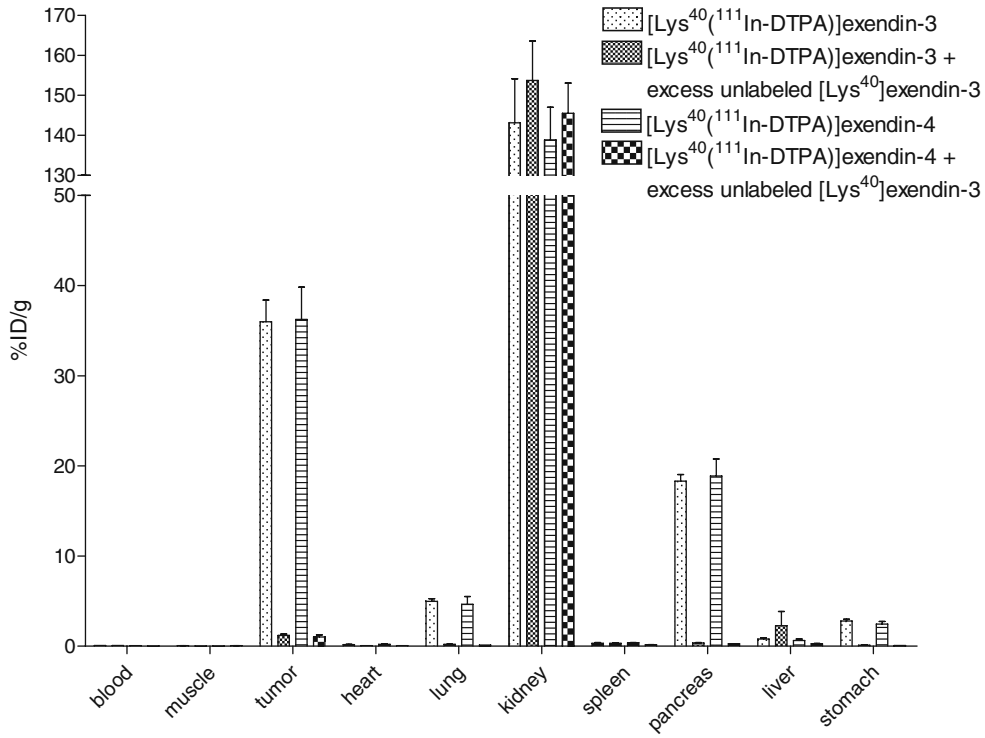

Fig. 4 Biodistribution of [Lys^{40}(^{111}In-DTPA)]exendin-3 and [Lys^{40} (^{111}In-DTPA)]exendin-4 in BALB/c nude mice bearing a subcutaneous INS-1 tumour. Values are mean percentage injected dose per gram tissue (n=5 mice, *error bars* SD). Blocking was performed by coinjection of a 100-fold molar excess of unlabelled [Lys^{40}]exendin-3. Mice were dissected 4 h after injection

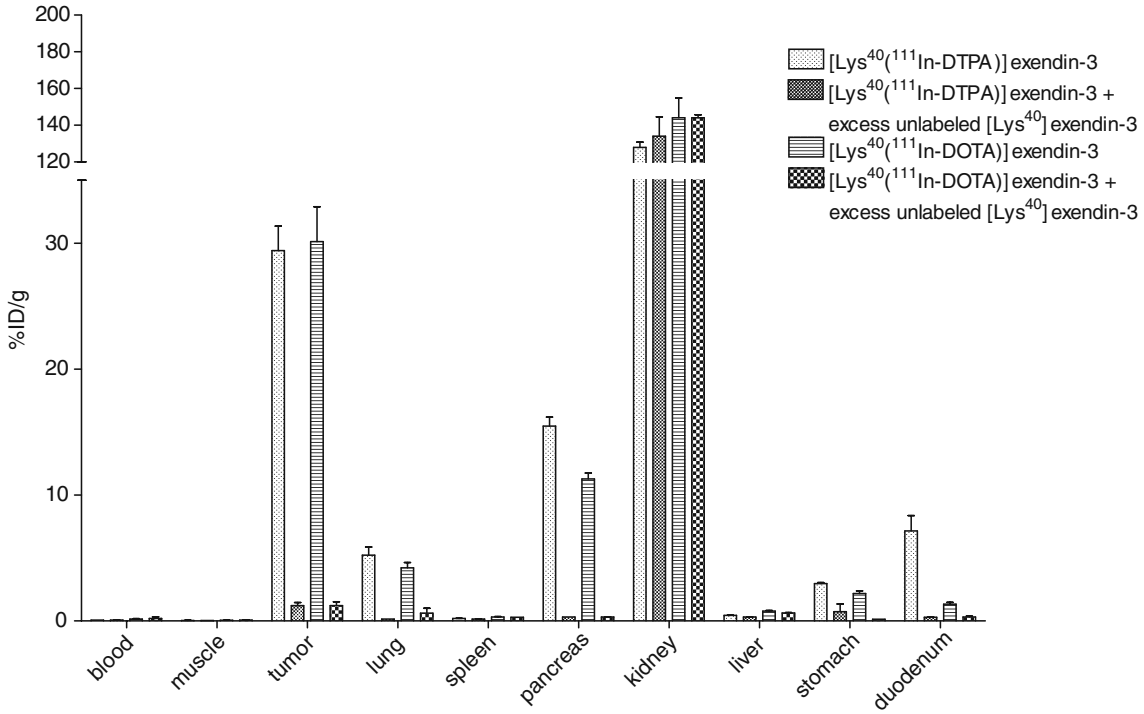

Fig. 5 Biodistributions of [Lys^{40}(^{111}In-DTPA)]exendin-3 and [Lys^{40}(^{111}In-DOTA)]exendin-3 in BALB/c nude mice bearing a subcutaneous INS-1 tumour. Values are mean percentage injected dose per gram tissue (n=5 mice, *error bars* SD). Blocking was performed by coinjection of a 100-fold molar excess of unlabelled [Lys^{40}]exendin-3. Mice were dissected 4 h after injection

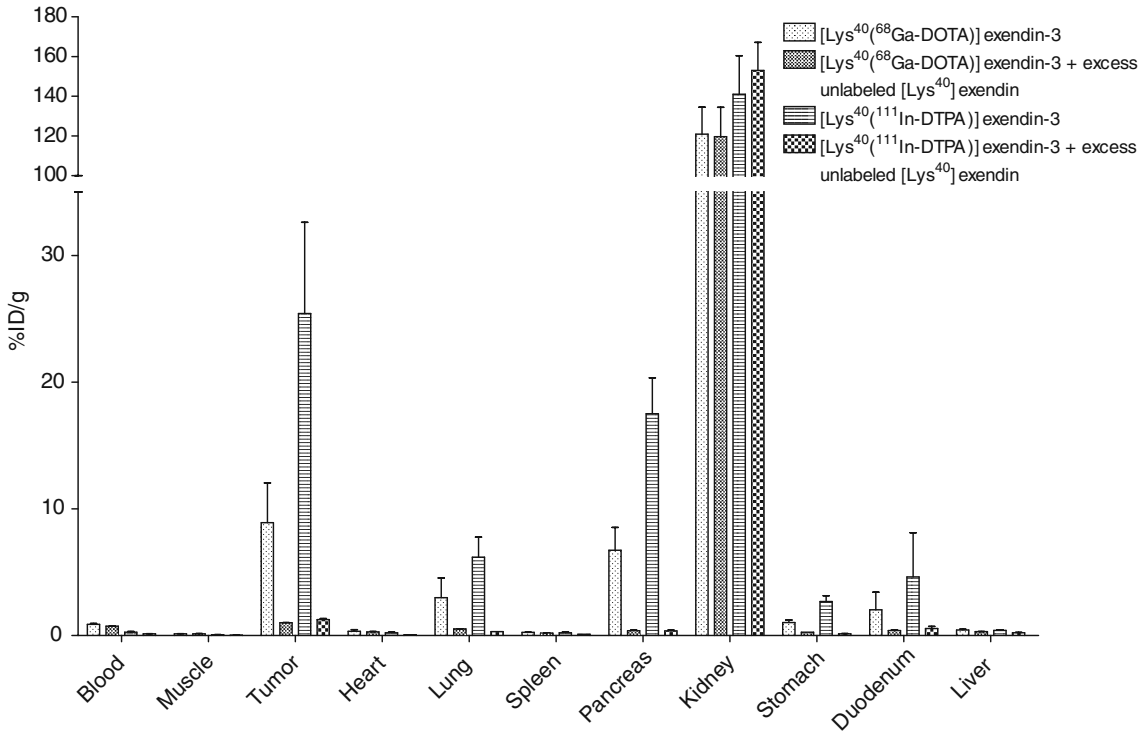

Fig. 6 Biodistributions of [Lys^{40}(^{111}In-DTPA)]exendin-3 and [Lys^{40}(^{68}Ga-DOTA)]exendin-3 in BALB/c nude mice bearing a subcutaneous INS-1 tumour. Values are mean percentage injected dose per gram tissue (n=5 mice, *error bars* SD). Blocking was performed by coinjection of a 100-fold molar excess of unlabelled [Lys^{40}]exendin-3. Mice were dissected 1 h after injection

with a subcutaneous INS-1 tumour using [Lys^{40}(^{111}In-DTPA)]exendin-3 as a reference (Fig. 6). Specific uptake of [Lys^{40}(^{68}Ga-DOTA)]exendin-3 was observed in tumour (p<0.05) and pancreas (p<0.05). Uptake of [Lys^{40}(^{68}Ga-DOTA)]exendin-3 was significantly lower than that of [Lys^{40}(^{111}In-DTPA)]exendin-3 in tumour (25.4±7.2%ID/g and 8.9±3.1 ID/g, p<0.01) and pancreas (17.5±2.8%ID/g and 6.7±1.8%ID/g, p<0.001).

In contrast to the RP-HPLC-purified preparation, [Lys^{40}(^{68}Ga-DOTA)]exendin-3 purified by gel filtration on a Sephadex G-25 column showed enhanced uptake in the spleen and liver (16.8±0.9%ID/g and 20.9±1.6%ID/g, respectively). This enhanced hepatic and splenic uptake was not receptor-mediated as it could not be blocked by coinjection of an excess of unlabelled [Lys^{40}]exendin (data not shown).Very low uptake in the liver and spleen was observed when RP-HPLC-purified [Lys^{40}(^{68}Ga-DOTA)]exendin-3 was injected (0.44±0.05%ID/g and 0.25±0.02%ID/g, respectively). Again, no specific uptake was observed in the liver and spleen as determined by coadministration of an excess of unlabelled exendin (0.31±0.02%ID/g and 0.20±0.01%ID/g, respectively).

Peptide dose escalation study

The effect of the exendin-3 dose on the biodistribution in mice with subcutaneous INS-1 tumours was studied in a peptide dose escalation study. The results of this study are summarized in Fig. 7. The highest uptake of [Lys^{40}(^{111}In-DTPA)]exendin-3 was observed when doses ≤0.1 μg of peptide were administered. Administration of 0.3 μg [Lys^{40}(DTPA)]exendin-3 resulted in a significantly reduced uptake of [Lys^{40}(^{111}In-DTPA)]exendin-3 in the tumour and the pancreas (p<0.0005 and p=0.001, respectively). Further escalation of the peptide dose resulted in a further decrease in tumour and pancreatic uptake of [Lys^{40}(^{111}In-DTPA)]exendin-3.

PET imaging

Subcutaneous INS-1 tumours in the hind limb were clearly visualized on the PET images as early as 1 h after injection

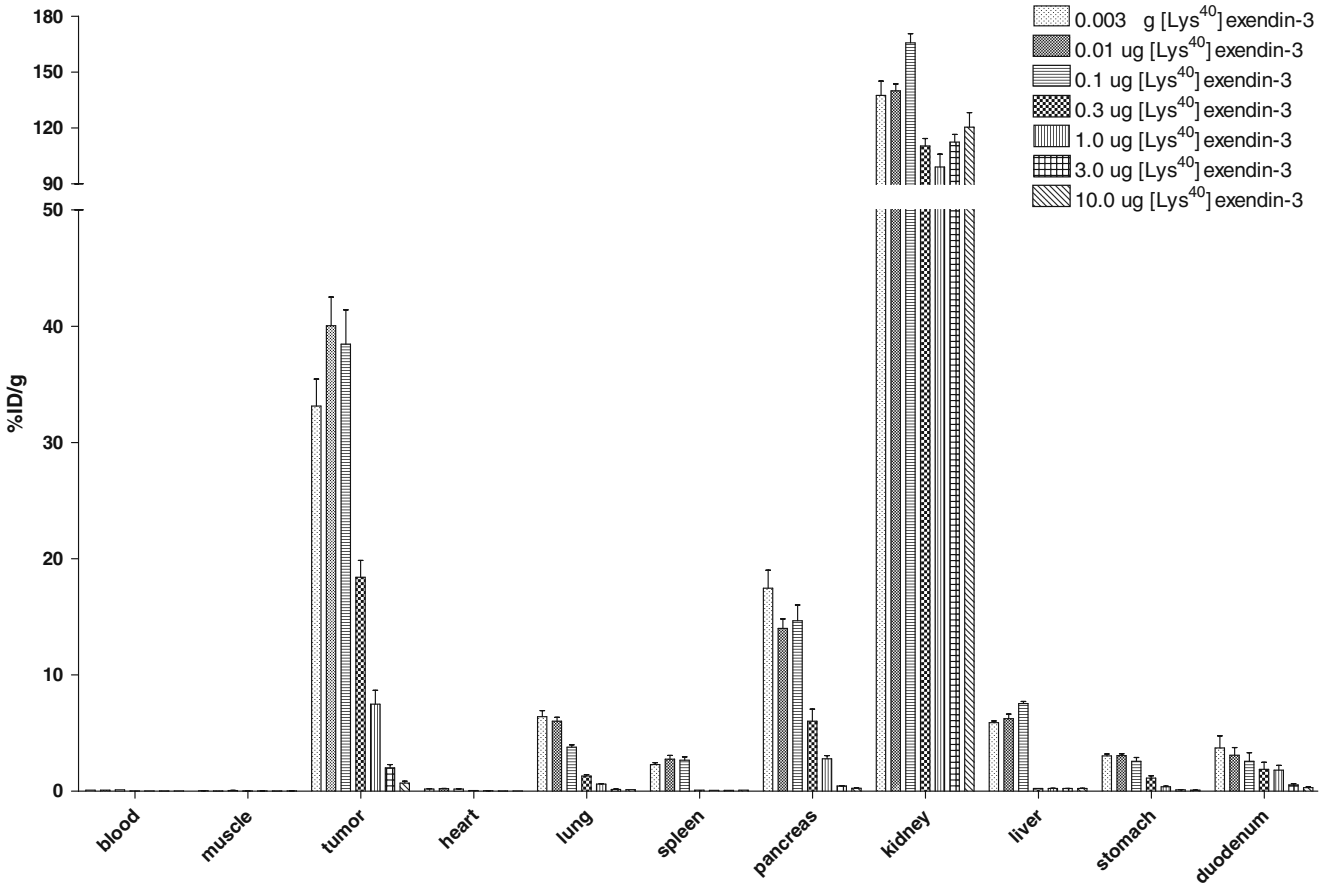

Fig. 7 Peptide dose escalation study of [Lys^{40}]exendin-3 in BALB/c nude mice with a subcutaneous INS-1 tumour. Mice were injected intravenously with 0.37 MBq [Lys^{40}(^{111}In-DTPA)]exendin-3 and were coinjected with various amounts of unlabelled [Lys^{40}]exendin 3 ranging from 0.003 to 10.0 μg. Values are mean percentage injected dose per gram tissue (n=5 mice, *error bars* SD). Mice were dissected 4 h after injection

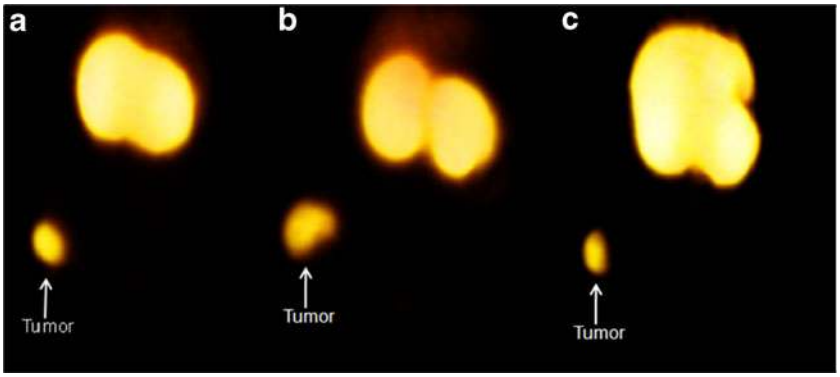

Fig. 8 Maximum intensity projection of PET images of different BALB/c nude mice with a subcutaneous INS-1 tumour in the right hind limb. **a**, **b** PET images of mice injected with HPLC-purified [Lys^{40}(^{68}Ga-DOTA)]exendin-3. The tumour (*arrows*) and kidneys are clearly visible. **c** PET image of mouse injected with unpurified [Lys^{40}(^{68}Ga-DOTA)]exendin-3. Although high uptake in the liver is seen, the tumour is still clearly visible

(Figs. 8 and 9). The PET images were fused with CT images. As well as high uptake in tumour, uptake was also seen in the kidneys. PET images following injection with unpurified [Lys^{40}(^{68}Ga-DOTA)]exendin-3 showed high uptake in the liver (Fig. 8c). Despite the high liver uptake tumours were still clearly visible.

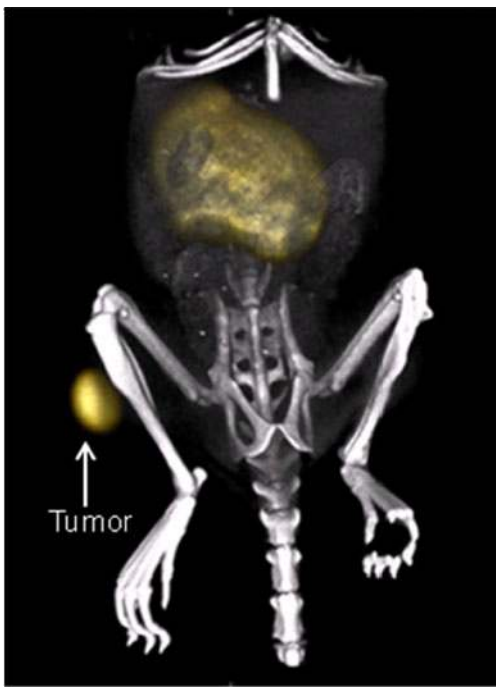

Fig. 9 Maximum intensity projection of a PET/CT image of a BALB/c nude mouse with a subcutaneous INS-1 tumour in the right hind limb after injection of 3 MBq HPLC-purified [Lys^{40}(^{68}Ga-DOTA)] exendin-3. The tumour (*arrow*) and kidneys are clearly visible. Due to the low background activity, the additional anatomical information given by the CT image helps to localize the tumour

Discussion

SRS, the standard method for imaging of NET, detects only around 50% of insulinomas [1, 2, 12]. Clinical studies with ^{18}F-DOPA PET for the detection of insulinomas have shown promising results [18]. However, physiological uptake of ^{18}F-DOPA in the pancreas and duodenum may cause false-positive results or mask small lesions. An exendin-based imaging method targeting the GLP-1R specifically expressed on insulinomas might therefore improve the visualization of insulinomas.

Preclinical studies with [Lys^{40}(^{111}In-DTPA)]exendin-4 in different animal models have shown high accumulation of ^{111}In-labelled exendin in insulinomas [12, 13]. Wild et al. demonstrated that in vivo imaging of insulinomas by SPECT with radiolabelled exendin is feasible in patients [15]. In a transgenic mouse model, they detected insulinomas of less than 1 mm in diameter using [Lys^{40}(^{111}In-DTPA)]exendin-4 as tracer. Although SPECT has a higher resolution in small-animal imaging, for clinical imaging PET offers a higher spatial resolution, a higher sensitivity and the possibility to accurately quantify uptake, which makes it preferable to SPECT. Recent studies have shown that PET imaging of NET with ^{68}Ga-labelled octreotide is superior to SPECT imaging with ^{111}In-labelled octreotide [19, 20].

In this study we therefore investigated the potential of [Lys^{40}(^{68}Ga-DOTA)]exendin-3 for the detection of insulinomas by PET in a mouse model. Conjugation of [Lys^{40}] exendin-3 with DOTA instead of DTPA allows radiolabelling of the tracer with a broad range of radionuclides including the positron emitter ^{68}Ga. We selected ^{68}Ga as positron emitter because it is a generator-derived radionuclide (and therefore readily available), the labelling strategy is fast and relatively simple, and the half-life matches the pharmacokinetics of the tracer (exendin) [13]. A potential

disadvantage of ^{68}Ga for animal imaging may be the high energy of the emitted β^+ particles limiting the spatial resolution of the images to 3 mm while the intrinsic resolution of the scanner is 1.5 mm [21]. This is only a relevant issue in preclinical scanners, as in clinical scanners the intrinsic resolution of the scanner rather than the β^+ energy will limit the resolution of the images.

Biodistribution studies in BALB/c nude mice with subcutaneous INS-1 tumours showed high and specific uptake of [Lys^{40}(^{68}Ga-DOTA)]exendin-3 in the tumour and pancreas. Subcutaneous INS-1 tumours in the hind limb of BALB/c nude mice were clearly visualized by microPET imaging. Therefore, our data show that imaging of insulinomas with ^{68}Ga-labelled exendin is feasible.

[Lys^{40}(^{111}In-DTPA)]exendin-3 was used as a reference in all experiments. Biodistribution studies with [Lys^{40}(^{111}In-DTPA)]exendin-3 showed specific uptake in GLP-1R-expressing tissues as described previously [13]. The peptide dose escalation study revealed that in this murine model a peptide dose of≤0.1 μg results in maximum accumulation of radiolabelled exendin in the tumour and in GLP-1R positive organs. Apparently, at higher doses in vivo receptors saturation occurs. The biodistribution of [Lys^{40}(^{111}In-DTPA)]exendin-3 was identical to the biodistribution of [Lys^{40}(^{111}In-DTPA)]exendin-4. Also there was no measurable effect of the chelator on receptor targeting as the biodistributions of [Lys^{40}(^{111}In-DTPA)]exendin-3 and [Lys^{40}(DOTA)]exendin-3 were identical.

The uptake of [Lys^{40}(^{68}Ga-DOTA)]exendin-3 in the tumour and the pancreas was significantly lower than that of [Lys^{40}(^{111}In-DTPA)]exendin-3. It has been demonstrated that the affinity of a peptide can be influenced by the chelator as well as by the radionuclide. Reubi et al. showed that ^{68}Ga-DOTA-TATE has a higher affinity for the somatostatin receptor subtype 2 than ^{111}In-DOTA-TATE [22]. However, there was no significant difference between the IC_{50} values of Lys^{40}(^{nat}In-DTPA)]exendin-3, [Lys^{40}(^{nat}In-DOTA)]exendin-3 and [Lys^{40}(^{nat}Ga-DOTA)]exendin-3. The differences in tumour and pancreatic uptake between [Lys^{40}(^{68}Ga-DOTA)]exendin-3 and [Lys^{40}(^{111}In-DTPA)]exendin-3 could not be attributed to the substitution of DTPA by DOTA, because in our mouse model, the uptakes of [Lys^{40}(^{111}In-DTPA)]exendin-3 and [Lys^{40}(DOTA)]exendin-3 in the tumour and other receptor-positive organs were identical.

Enhanced uptake of [Lys^{40}(^{68}Ga-DOTA)]exendin-3 was seen in the liver and spleen when the preparation was only purified by gel filtration, probably because this preparation still contained some colloidal ^{68}Ga. Colloidal ^{68}Ga will accumulate in the liver and spleen. RP-HPLC purification removed the colloidal contamination, since this preparation had the same very low uptake in the liver and spleen as the ^{111}In-labelled preparation. Previous studies with ^{68}Ga-labelled DOTA-conjugated compounds not purified by RP-HPLC have also shown enhanced liver and spleen uptake [23, 24]. It is still a matter of debate whether the enhanced uptake in liver and spleen is caused by colloidal ^{68}Ga or by instability of the ^{68}Ga-DOTA complex. In the present study, uptakes of HPLC-purified [Lys^{40}(^{68}Ga-DOTA)]exendin-3 in the liver and spleen were identical to that of ^{111}In-labelled exendin-3. Our data suggest that the enhanced uptake in the liver and spleen of ^{68}Ga-labelled compounds found in previous studies is not caused by instability of the ^{68}Ga-DOTA complex but by minor amounts of colloid.

To obtain high-quality PET images a ^{68}Ga activity of 3 MBq was required. This necessitated the administration of an exendin dose of 0.3 μg, and although this resulted in suboptimal uptake (as demonstrated in the peptide dose escalation study), the tumours could exactly be visualized.

GLP-1R is also expressed on native pancreatic beta-cells. Radiolabelled exendin can potentially be used to target beta-cells. This is an attractive approach for the determination of beta-cell mass, a key issue in diabetes mellitus. [Lys^{40}(^{111}In-DTPA)]exendin and [Lys^{40}(^{68}Ga-DOTA)]exendin potentially can be used to noninvasively determine the beta-cell mass in the pancreas by SPECT or PET. A previous study has shown a correlation between the uptake of ^{111}In-labelled exendin and the beta-cell mass [25], which makes this approach promising for the in vivo determination of the beta-cell mass.

In conclusion, ^{68}Ga-labelled [Lys^{40}(DOTA)]exendin-3 is a suitable tracer for PET imaging of GLP-1R-expressing insulinomas. ^{68}Ga-labelled [Lys^{40}(DOTA)]exendin-3 showed high uptake in subcutaneous INS tumours in BALB/c mice. Subcutaneous INS-1 tumours were clearly visualized with a microPET/CT scanner after injection of ^{68}Ga-labelled [Lys^{40}(DOTA)]exendin-3. Therefore, clinical studies should be conducted to elucidate the potential of [Lys^{40}(^{68}Ga-DOTA)]exendin-3 for insulinoma imaging in humans.

Acknowledgments This work was supported by NIH grant 1R01 AG 030328-01.

References

1. Modlin IM, Tang LH. Approaches to the diagnosis of gut neuroendocrine tumors: the last word (today). Gastroenterology 1997;112:583–90.
2. Krenning EP, Kwekkeboom DJ, Bakker WH, Breeman WA, Kooij PP, Oei HY, et al. Somatostatin receptor scintigraphy with [111In-

DTPA-D-Phe1]- and [123I-Tyr3]-octreotide: the Rotterdam experience with more than 1000 patients. Eur J Nucl Med 1993;20:716–31.
3. Joseph K, Stapp J, Reinecke J, Skamel HJ, Hoffken H, Benning R, et al. Receptor scintigraphy using 111In-pentetreotide in endocrine gastroenteropancreatic tumors. Nuklearmedizin 1993;32:299–305.
4. Abboud B, Boujaoude J. Occult sporadic insulinoma: localization and surgical strategy. World J Gastroenterol 2008;14:657–65.
5. Jackson JE. Angiography and arterial stimulation venous sampling in the localization of pancreatic neuroendocrine tumours. Best Pract Res Clin Endocrinol Metab 2005;19:229–39.
6. Reubi JC, Waser B. Concomitant expression of several peptide receptors in neuroendocrine tumours: molecular basis for in vivo multireceptor tumour targeting. Eur J Nucl Med Mol Imaging 2003;30:781–93.
7. Gotthardt M, Fischer M, Naeher I, Holz JB, Jungclas H, Fritsch HW, et al. Use of the incretin hormone glucagon-like peptide-1 (GLP-1) for the detection of insulinomas: initial experimental results. Eur J Nucl Med Mol Imaging 2002;29:597–606.
8. Singh G, Eng J, Raufman JP. Use of 125I-[Y39]exendin-4 to characterize exendin receptors on dispersed pancreatic acini and gastric chief cells from guinea pig. Regul Pept 1994;53:47–59.
9. Hassan M, Eskilsson A, Nilsson C, Jonsson C, Jacobsson H, Refai E, et al. In vivo dynamic distribution of 131I-glucagon-like peptide-1 (7-36) amide in the rat studied by gamma camera. Nucl Med Biol 1999;26:413–20.
10. Gotthardt M, Boermann OC, Behr TM, Behe MP, Oyen WJ. Development and clinical application of peptide-based radiopharmaceuticals. Curr Pharm Des 2004;10:2951–63.
11. Goke R, Larsen PJ, Mikkelsen JD, Sheikh SP. Distribution of GLP-1 binding sites in the rat brain: evidence that exendin-4 is a ligand of brain GLP-1 binding sites. Eur J Neurosci 1995;7:2294–300.
12. Wild D, Behe M, Wicki A, Storch D, Waser B, Gotthardt M, et al. [Lys40(Ahx-DTPA-111In)NH2]exendin-4, a very promising ligand for glucagon-like peptide-1 (GLP-1) receptor targeting. J Nucl Med 2006;47:2025–33.
13. Gotthardt M, Lalyko G, van Eerd-Vismale J, Keil B, Schurrat T, Hower M, et al. A new technique for in vivo imaging of specific GLP-1 binding sites: first results in small rodents. Regul Pept 2006;137:162–7.
14. Wicki A, Wild D, Storch D, Seemayer C, Gotthardt M, Behe M, et al. [Lys40(Ahx-DTPA-111In)NH2]-Exendin-4 is a highly efficient radiotherapeutic for glucagon-like peptide-1 receptor-targeted therapy for insulinoma. Clin Cancer Res 2007;13:3696–705.
15. Wild D, Macke H, Christ E, Gloor B, Reubi JC. Glucagon-like peptide 1-receptor scans to localize occult insulinomas. N Engl J Med 2008;359:766–8.
16. Asfari M, Janjic D, Meda P, Li G, Halban PA, Wollheim CB. Establishment of 2-mercaptoethanol-dependent differentiated insulin-secreting cell lines. Endocrinology 1992;130:167–78.
17. Laverman P, Roosenburg S, Gotthardt M, Park J, Oyen WJ, de Jong M, et al. Targeting of a CCK(2) receptor splice variant with (111)In-labelled cholecystokinin-8 (CCK8) and (111)In-labelled minigastrin. Eur J Nucl Med Mol Imaging 2008;35:386–92.
18. Kauhanen S, Seppanen M, Minn H, Gullichsen R, Salonen A, Alanen K, et al. Fluorine-18-L-dihydroxyphenylalanine (18F-DOPA) positron emission tomography as a tool to localize an insulinoma or beta-cell hyperplasia in adult patients. J Clin Endocrinol Metab 2007;92:1237–44.
19. Buchmann I, Henze M, Engelbrecht S, Eisenhut M, Runz A, Schafer M, et al. Comparison of 68Ga-DOTATOC PET and 111In-DTPAOC (Octreoscan) SPECT in patients with neuroendocrine tumours. Eur J Nucl Med Mol Imaging 2007;34:1617–26.
20. Kowalski J, Henze M, Schuhmacher J, Macke HR, Hofmann M, Haberkorn U. Evaluation of positron emission tomography imaging using [68Ga]-DOTA-D Phe(1)-Tyr(3)-octreotide in comparison to [111In]-DTPAOC SPECT. First results in patients with neuroendocrine tumors. Mol Imaging Biol 2003;5:42–8.
21. van Dalen JA, Visser EP, Laverman P, Vogel WV, Oyen WJG, Corstens FHM, et al. Effect of the positron range on the spatial resolution of a new generation pre-clinical PET using fluorine-18, gallium-68, zirconium-89 and iodine-124. Eur J Nucl Med Mol Imaging 2007;34:S228-S.
22. Reubi JC, Schar JC, Waser B, Wenger S, Heppeler A, Schmitt JS, et al. Affinity profiles for human somatostatin receptor subtypes SST1-SST5 of somatostatin radiotracers selected for scintigraphic and radiotherapeutic use. Eur J Nucl Med 2000;27:273–82.
23. Antunes P, Ginj M, Zhang H, Waser B, Baum RP, Reubi JC, et al. Are radiogallium-labelled DOTA-conjugated somatostatin analogues superior to those labelled with other radiometals? Eur J Nucl Med Mol Imaging 2007;34:982–93.
24. Breeman WA, de Jong M, de Blois E, Bernard BF, Konijnenberg M, Krenning EP. Radiolabelling DOTA-peptides with 68Ga. Eur J Nucl Med Mol Imaging 2005;32:478–85.
25. Brom M, Baumeister P, Melis M, Laverman P, Joosten L, Behe M, et al. Determination of the beta-cell mass by SPECT imaging with In-111-DTPA-Exendin-3 in rats. J Nucl Med 2009;50(Suppl 2):147.